1-1-2009

Removal of boron, fluoride and nitrate by electrodialysis in the presence of organic matter

Laura J. Banasiak
University of Wollongong, lbanasia@uow.edu.au

Andrea I. Schafer
University of Edinburgh

Removal of boron, fluoride and nitrate by electrodialysis in the presence of organic matter

Laura J. Banasiak and Andrea I. Schäfer

School of Engineering and Electronics, The University of Edinburgh, Edinburgh, EH9 3JL, United Kingdom

Ph: +44 (0) 131 650 7209; Fax: +44 (0) 131 650 6781; Email: Andrea.Schaefer@ed.ac.uk

Submitted to

Journal of Membrane Science

June 2008

Revision submitted:

January 2009

Abstract

The removal of the trace inorganic contaminants boron ($B(OH)_4^-$), fluoride (F^-) and nitrate (NO_3^-) from synthetic aqueous solutions containing organic matter using electrodialysis was investigated. The transport of the contaminants through the ion-exchange membranes was evaluated in relation to hydrated ionic radius, whereby a positive correlation was found in absence of organic matter. NO_3^-, with the smaller hydrated ionic radius and weaker hydration shell, was removed more effectively than F^-, which has a larger hydrated ionic radius and stronger hydration shell. The removal of F^- and NO_3^- was not significantly influenced by solution pH due to their pH independent

speciation. However, the removal of boron was dependent on increasing solution pH and the degree of demineralization. Dissolved organic matter (humic acid, tannic acid and alginic acid) resulted in enhanced removal of boron and F^- as a result of the binding of F^- within the organic matter structure and complexation of boric acid ($B(OH)_3$) with carboxylate groups in the organic matter. Deposition of organic matter to the anion-exchange membranes was noted. Inorganic trace contaminant and organic matter membrane deposition influenced system performance in regards to an increase in stack resistance and decrease in removal and flux of total dissolved solids.

Keywords: Electrodialysis; Ion transport; Inorganic trace contaminant removal; Dissolved organic matter; Fouling; Groundwater/Brackish water

1. Introduction

Membrane processes such as electrodialysis (ED) are increasingly being utilised in water treatment to remove dissolved contaminants. A wide range of inorganic trace contaminants, including fluoride (F^-) and nitrate (NO_3^-), can be found in surface, brackish and groundwater. The occurrence and fate of these contaminants is an environmental and public health concern. Concentrations of F^- in surface water are relatively low (<0.1–0.5 mg/L) [1], while concentrations up to 20 mg/L have been found in groundwater [2]. The harmful effects of excess F^- (dental and skeletal fluorosis) have been widely studied [3, 4]. NO_3^- concentrations in surface and groundwater have increased worldwide due to heavy utilization of artificial fertilizers [5]. Deleterious health effects due to NO_3^- include infantile methemoglobinaemia (known as ‘blue-baby’ syndrome) and cancer risks for adults and older children [5]. According to the World Health Organization (WHO) [1], the European Union (EU) Drinking Water Directive [6] and the Australian Drinking Water Guidelines (ADWG) [7], the maximum levels for F^- and NO_3^- in drinking water are 1.5 and 50 mg/L, respectively. However, for NO_3^- a level of 25 mg/L has been recommended [1, 7]. Due to its high selectivity and low chemical demand, ED has proved an efficient method for desalination and the removal of F^- and NO_3^- [8, 9].

Boron is another contaminant of interest due to its occurrence in seawater and difficulty of removal in desalination. While natural concentrations in surface and groundwaters are usually low, concentrations up to 100 mg/L have been found as a result of wastewater discharge [10]. Long-term consumption of water and food products with increased boron content results in malfunctioning of cardiac-vascular, nervous, and alimentary systems of humans [11]. The WHO and EU Council have set limits of 0.5 mg/L and 1 mg/L for drinking water, respectively [1, 6]. Boron removal using ED has previously been studied [12, 13]; however its interaction with organic matter (OM) and the subsequent impact on its removal has not been investigated. ED is capable of removing 42 – 75 % of boron, with removal efficiency dependent on solution pH (97 % at pH 9 - 10) and the degree of desalination [10, 13]. In acidic and near neutral aqueous environments boron is mainly present as $B(OH)_3$ and partially as borate ions according to the dissociation reaction (Ka = 6×10^{-10}, pKa 9.24 at 25°C) [14]:

$$B(OH)_3 + H_2O \rightleftharpoons B(OH)_4^- + H^+ \qquad \textbf{(1)}$$

Organic matter (OM) occurs in aquatic ecosystems in concentrations of 0.5 to 100 mgC/L [15] and have been a focal point in water treatment research as they are precursors to disinfection by-products. Dissolved organic substances (e.g. humic substances) act as ligands for metal ions, oxides hydroxides, minerals and organic micropollutants and form water-soluble and water-insoluble complexes [16]. Organic matter comes with seasonal and location (origin) specific characteristics and hence it is important to consider diverse groups such as humics, polyphenols, and polysaccharides.

In ED, organic substances, such as humate, deposit on the ion-exchange membranes and can cause increases in electrical resistance of the membranes [17]. HA in particular has been reported to be

responsible for fouling in ED which affects salt flux [18-20]. As most OM is negatively charged at neutral pH, deposits form predominantly on the anion exchange membranes. The impact of such deposits on removal of specific contaminants is not well understood. Further, solute-solute interactions (such as complexation) of OM with inorganic compounds ($B(OH)_4^-$, F^- and NO_3^-) has to date not been investigated. As such interactions are likely to affect removal, the main objective of this study was to examine the influence of pH and three types of OM on the removal of $B(OH)_4^-$, F^- and NO_3^- during ED systematically. In order to achieve this goal the project was conducted in five stages, namely (1) mechanisms of inorganics removal (in absence of OM), (2) OM removal, (3) impact of OM on inorganics removal, (4) inorganic membrane deposit formation, and (5) organic deposit formation.

2. Materials and Methods

2.1. Chemicals and solution preparation

The feed solution (diluate and concentrate, 4L each) was prepared by dissolving ACS reagent grade NaCl (5 g/L) and $NaHCO_3$ (84 mg/L) (Fisher Scientific UK), NaF (5 mg/L; total mass 2.1 mmol), $NaNO_3$ (100 mg/L; total mass 57 mmol) and H_3BO_3 (10 mg/L; total mass 7.4 mmol) (Sigma Aldrich UK) in ultrapure water. The concentrations of H_3BO_3, F^- and NO_3^- were selected within the range found in brackish waters [12, 21]. Experiments with an identical concentration of 10 mg/L for H_3BO_3, F^- and NO_3^- as well as detailed investigation of the pH range 8.5 to 9.5 for the initial NaCl concentrations of 5 g/L and 20 g/L (results not shown). Data on hydrated ionic radii and hydration energy are outlined in Table 1.

[Table 1]

98 Na_2SO_4 (99 % purity) was used in the electrode rinse solution (Fisher Scientific UK) and analytical
99 grade reagents NaOH and HCl (Fisher Scientific UK) were used for pH adjustments and membrane
100 cleaning.
101
102 Three different types of OM were selected for use in this study: humic acid sodium salt (HA),
103 tannic acid (TA) and alginic acid sodium salt (AA) (all Sigma Aldrich UK). The concentration of
104 OM in different waters is highly variable [15] and hence an average OM concentration of 12.5
105 mgC/L was used in all experiments. The respective OM solutions were prepared by dissolving HA,
106 TA and AA in ultrapure water and adding them to the feed solution. Physical and chemical
107 properties of the OM compounds are outlined in Table 2.
108
109 [Table 2]
110
111 Major functional groups of HA include carboxylic, phenolic, alcohol/aldehyde acids, and methoxyl
112 and HA is negatively charged at neutral pH [22]. As a polyphenol, TA can form inter- and
113 intramolecular hydrogen bonds and often exists in solution as loosely bound complexes of
114 molecules [23]. At acidic pH TA is neutrally charged, however as pH increases the charge becomes
115 negative [24]. AA is a naturally occurring hydrophilic colloidal polysaccharide, is obtained from
116 brown seaweed and exhibits negatively charged carboxylate and neutral hydroxyl groups at pH 7
117 [25]. Below pH 4, the charge density decreases causing increased aggregation, whereas above pH 8
118 dissociation has been observed [26].
119
120 *2.2. Electrodialysis System*
121 The ED stack used was a BEL-500 unit (Berghof, Germany) with seven Neosepta CMX-SB cation-
122 exchange membranes (CEMs) and six Neosepta AMX-SB anion-exchange membranes (AEMs)
123 (supplied by Eurodia, Germany; manufactured by Astom Corporation, Tokyo, Japan) with an

available membrane area of 58 cm^2 each. The ED cell was connected to a DC electric potential (GW Instek DC Power supply Model GPR-1810HD, Taiwan) through TiO_2-coated titanium electrodes. A schematic of the ED system is shown in Figure 1.

[Figure 1]

The limiting current density (LCD, 7.8 mA/cm^2) was derived from a set of current-voltage curves measured in the ED cell and in consequence the applied voltage fixed to 10V to operate below the LCD. Diluate and concentrate were recirculated through the ED cell at a flow rate of 1.5 L/min until the desired product concentration (0.5 g/L NaCl) was achieved in the diluate. 0.5 mol/L Na_2SO_4 was used as an electrode rinse solution at a flow rate of 1.5 L/min, in order to prevent the generation of chlorine or hypochlorite, which could be hazardous for the electrodes, had NaCl been used instead.

The resistance across the ED stack was calculated using Ohms law:

$$R = \frac{E}{I} \quad \textbf{(2)}$$

Where, R is the resistance (Ohm), E the electrical potential (Volt) and I the electrical current (Ampere).

2.3. Analytical Methods

The pH, electrical conductivity (EC) and temperature of samples taken from the diluate and concentrate during each experiment was measured using a pH/Conductivity meter (Multiline P4 combination pH electrode, WTW Germany).

F^- and NO_3^- concentrations were determined using ion-selective electrodes (ISE) in conjunction with a standard reference electrode connected to a Metrohm 781 Ion Meter (UK). The ISEs were

150 regularly calibrated, with and without OM, and cleaned using standard methods. Standards and
151 samples were mixed with a total ionic strength adjustment buffer (TISAB) to avoid possible
152 interferences resulting from changes in solution pH and conductivity**.** NO_3^- sample analysis was
153 checked using a Quickchem 8500 FIA Nutrient Analyser (Lachat Instruments, Colorado, USA) and
154 F^- analysis was verified using a DX-500 ion chromatograph (DIONEX, Sunnyvale, CA, USA).
155 Sample concentrations were in agreement with ISE results. Total concentrations of H_3BO_3 were
156 determined by ICP-OES using a Perkin Elmer Optima 5300DV instrument (Perkin Elmer, UK).
157
158 UV-Visible Spectrometry (Varian Cary 100 Scan, UK) was utilized to determine the absorbance of
159 OM in experimental samples. HA was analyzed at a wavelength of 254 nm, whereas TA and AA
160 were analyzed at wavelengths of 275 nm and 198 nm, respectively. Specific UV absorbance
161 (SUVA, L/mg.m) values were calculated for HA as in equation (2):

162 $$\text{SUVA} = \frac{\text{UV Abs(/m)}}{\text{DOC (mgC/L)}} \times 100 \qquad \textbf{(2)}$$

163
164 Non-purgeable organic carbon (NPOC) concentrations were determined using a total organic
165 carbon analyser (Shimadzu TOC-VCPH, UK).
166
167 The mass of contaminants deposited on the membranes was calculating using a mass balance:

168 $$M_{Dep} = M_F - M_D - M_C \qquad \textbf{(3)}$$

169 where M_{Dep} is deposit, M_F feed, M_D diluate and M_C concentrate mass (mmol for H_3BO_3, F^-, NO_3^-),
170 respectively.
171
172 *2.4. Experimental Protocol*
173 Concentrate and diluate pH was maintained constant during the experiments and adjusted by the
174 addition of 1 mol/L HCl and/or NaOH in the range of pH 3-12. EC of both solutions was
175 continuously monitored and samples were collected at the beginning and at 20 minute intervals for

176 analyses of H_3BO_3, F^-, NO_3^-, UV-Vis absorbance and non-purgeable organic carbon (NPOC). After
177 the completion of each experiment, cleaning solutions of 0.1 mol/L HCl, 0.1 mol/L NaOH and
178 ultrapure water were circulated through the ED cell for 20 minutes each in order to remove any
179 deposits. Samples taken from the cleaning solutions were analysed for UV-Vis absorbance and
180 NPOC. After each set of OM experiments, the ED cell was dismounted and photographs were taken
181 of the anion- and cation-exchange membranes.
182
183 Ion and EC removal (R_D, %) from the diluate was calculated using eqn (4):

184 $$R_D = \frac{\left(C_{Di}^0 - C_{Di}^T\right)}{C_{Di}^0} \times 100\% \quad \textbf{(4)}$$

185 where, C_{Di}^0 is the initial diluate ion concentration or EC and C_{Di}^T is the diluate ion concentration or
186 EC in the time period T (hours). Average ion and EC removal (%) was calculated along with
187 standard deviation (± %). Note that ion removal includes deposit formation, while the flux of ions
188 and EC (J_i, mmol/m^2.h for ions and mS/cm/m^2.h for EC) across the membranes was calculated
189 using eqn (5):

190 $$J_i = \frac{\left(C_{Ci}^T - C_{Ci}^0\right)}{A_m T} \quad \textbf{(5)}$$

191 where, C_{Ci}^T (mmol for $B(OH)_4^-$, F^- and NO_3^-, mS/cm for EC) is concentrate mass (ions) in the
192 concentrate in the time period T, C_{Ci}^0 is the initial mass within the concentrate and A_m is the
193 membrane area (m^2) used in the transport of the respective ion.
194
195 **3. Results and Discussion**
196 *3.1. Inorganic trace contaminant removal*
197 As a first stage the removal of ions in the absence of OM was determined to establish a baseline.
198 The removal of F^- from the diluate is shown in Figure 2A. The removal of F^- was independent of

pH, which is due to the pH independence of F^- speciation [27]. F^- ions removal was 65.6 ± 12.0 %, while F^- flux was approximately 10 mmol/m^2.h (see Figure 3A).

[Figure 2]

[Figure 3]

Removal of NO_3^- is higher than that of F- but equally pH independent (Figure 2B), again because NO3- speciation does not vary over the pH range studied [28]. The average removal of NO3- was 94.1 ± 1.3 % while NO3- flux was significantly higher than for F- and decreased gradually from 830 to 408 mmol/m2.h (Figure 3B).

$B(OH)_3$ does not dissociate at pH 3-8 and in consequence is not transported effectively through the AEM (see Figure 2C). Above pH 9 removal increases to 61.2 % at pH 12 due to $B(OH)_3$ dissociation and speciation hence plays an important role. While Yazicigil *et al.* [13] determined that pH 9 was the optimal point for $B(OH)_4^-$ removal, in this study it was only 13.7 % at pH 9. $B(OH)_4^-$ flux is in the same order of magnitude as F- but increased during experiments (see Figure 3C) which confirms the findings of Yazicigil et al. who attributed this to the increase in electrochemical potentials gradient between the diluate and concentrate (i.e. larger difference in salt concentration) [13]. The dissociation constant of $B(OH)_3$ decreases with increasing NaCl concentration [29]. Further ED experiments were undertaken to examine this effect with a solution pH range between 8.5 and 9.5 (insert Figure 2D) at two feed NaCl concentrations of 5 and 20 g/L NaCl. In the 5 g/L experiment $B(OH)_4^-$ removal ranged from 6.1 % at pH 8.5 to 29.4 % at pH 9.5. $B(OH)_4^-$ was not removed over this pH range in the 20 g/L experiment presumably due to the higher concentration of competitive ions within the diluate. In consequence, no discernable shift in

224 the dissociation constant of $B(OH)_3$ was observed. The results demonstrate however that NaCl
225 concentration affects removal of other ions.
226
227 The ionic characteristics (Table 1) can be used to explain differences in the transport (removal and
228 flux) of F^- and NO_3^- through the ion-exchange membranes. As no data was available on the
229 hydrated radius of $B(OH)_4^-$, comparison of $B(OH)_4^-$ removal and ionic characteristics is not
230 discussed. Ions with smaller intrinsic crystal radii have higher hydration numbers, larger hydrated
231 radii and hold their hydration shells more strongly [30], as illustrated in Figure 4. The crystal ionic
232 radius of F^- is 0.116 nm compared with 0.179 nm for NO_3^-. The larger the crystal ionic radius the
233 more diffuse the electric charge and the fewer water molecules surround the ion [31]. Therefore,
234 NO_3^- ions are less hydrated than F^- ions may separate from its hydration layer [30] and transport
235 through the ion-exchange membranes more easily.
236
237 The strength of hydration of F^- and NO_3^- is quantified by the Gibbs energy of hydration and the
238 number of water molecules within their hydration shells. NO_3^- has a lower Gibbs free energy (-275
239 kJ/mol compared to -345 kJ/mol for F^-). While it is to date not understood if water molecules
240 separate from their ions during transport through ion-exchange membranes, it is hypothesised that
241 separation is possible if the 'transport energy' is greater than the Gibbs free energy that bonds the
242 hydrated shell to the ion.
243
244 [Figure 4]
245
246 Ion mobility ionic permeabilities [32] further influence transport through ion-exchange membranes.
247 The ionic mobility of NO_3^- in solution (7.4×10^{-8} m^2/sV) solution is greater than the ionic mobility
248 of F^- (5.7×10^{-8} m^2/sV) [33]. The current passing through an ionic solution in ED and the resultant
249 transport of ions is related to the conductivity of the ionic solutions. The ion equivalent conductivity

of NO_3^- (71.5 $cm^2/\Omega.equiv$) is also greater than that of F^- (55.4 $cm^2/\Omega.equiv$), all factors contributing to higher flux of NO_3^- than F^-. To confirm those results independent of their concentration, an experiment with the same initial mass concentration for boron, F^- and NO_3^- (10 mg/L at pH 10) was carried out. The removal of NO_3^- was 95.3 % compared with 76.2 % for F^-, further indicating that NO_3^- with the smaller hydrated radius is removed more efficiently than F^- with the larger hydrated radius.

3.2. Organic matter removal

Figure 5 shows the removal of OM as a function of solution pH in diluate and concentrate. The fact that OM is removed from both compartments indicates that this removal is a deposition on the membrane rather than transport through the membrane. However, staining of the membranes indicates that membrane penetration also occurs. Removal of AA from the diluate is low with an average of 9.2 ± 1.6 % and independent of pH given its negative charge at pH 3-12. The removal of HA and TA from the diluate is higher with an average removal of 19.1 ± 3.7 % and 19.8 ± 9.5 %, respectively. While HA removal is pH independent, the removal of TA increased with pH to 44.3 % at pH 12 due to its increasing negative charge. Removal of OM from the concentrate was less than from the diluate due to electrostatic repulsion with the negatively charged functional groups in the CEMs adjacent to the concentrate compartment. This confirms the results of Park et al. who found that deposits occur mostly on the diluate side of AEM membranes.

[Figure 5]

3.3. Effect of organic matter on inorganic trace contaminant removal

Organic matter (OM) deposits on the membranes and interacts with inorganic contaminants. The removal of F^- was greater in the presence of OM (Figure 2A), which can be attributed to the binding of F^- to the OM [16]. The average percentage of F^- ions removed with TA was 74.8 ± 6.0 %,

followed by AA and HA with 72.9 ± 5.8 % and 72.5 ± 4.5 % respectively. The flux of F^- was reduced in the presence of OM. The final flux (after 140 minutes) was 10.0 mmol/m^2.h, 8.6 mmol/m^2.h and 9.4 mmol/m^2.h with HA, TA and AA, respectively compared to 10.7 mmol/m^2.h in the absence of OM. Combined increase in removal and reduced flux indicates F^- membrane deposition.

No significant difference in NO_3^- due to OM; HA (91.9 ± 3.5 %), TA (91.4 ± 4.9 %) and AA (92.6 ± 0.8 %) removal was observed. For experiments with TA, NO_3^- removal was highest under acidic-neutral pH conditions (95.2 - 93.2 % at pH 3 - 7). In HA experiments, NO_3^- removal was pH independent while the flux of NO_3^- (Figure 3B) was reduced in the presence of OM. This again demonstrated some degree of membrane deposition.

The presence of OM also enhanced boron removal between pH 3 and 8 (Figure 2C) while above pH 9, the removal of $B(OH)_4^-$ in the presence of OM was lower. $B(OH)_4^-$ flux at high pH was lower in the presence of OM (Figure 3C), and again results indicate $B(OH)_4^-$-OM complexation and $B(OH)_4^-$ membrane deposition.

3.4. Inorganic trace contaminant membrane deposition

The deposit formation can be quantified using mass balance. The mass of F^- deposited on the membranes is shown in Figure 6A, with negligible deposition in experiments without OM. In the presence of OM the mass of F^- deposited was between 0.1 and 0.6 mmol (4.7 and 28.8 % initial mass); with a greater amount deposited with HA and TA. HA contains voids which can trap inorganic compounds [34] and binding of F^- has been shown to be pH dependent [16]. Hayes [16] studied the binding of F^- to HA as a function of solution pH (5.0 - 6.6) and in this narrow pH range F^- was being trapped within the large structure of HA rather than bound to a particular functional group. As solution pH increases HA deprotonates and the negative charge on the carboxylates

repels the F^- ion. This phenomenon was not observed in this current study due to the fact that the adsorption of F^- in ED would be governed by several other factors (e.g. presence of other contaminants).

The mass of NO_3^- deposited on the membranes was greater in experiments with OM (Figure 6B) with values of between 4.6 and 13.8 mmol (8.1 and 24.2 % initial mass). Contrary to the negative charge of HA above pH 5 (Table 2) the mass of NO_3^- adsorbed to the membranes in the presence of HA increased above pH5. Adsorption of NO_3^- in experiments with TA was independent of pH. In the presence of AA, the mass of NO_3^- adsorbed was lower at pH 6 - 8 because repulsion between the negatively charged AA and NO_3^- would be expected.

The mass of $B(OH)_4^-$ deposited on the membranes is greater in experiments with OM (Figure 6C) with values of between 0.3 and 1.4 mmol (4.0 and 19.0 % initial mass). Removal of $B(OH)_3$ between pH 3 and 8 (Figure 2C) may be the result of $B(OH)_3$ complexation with polar organic compounds [35], such as HA. Schmitt-Kopplin *et al*. [36] postulated that $B(OH)_3$ binds to carboxylate groups (COO^-) within HA where it forms a transient hydrogen bonded structure with the HA. A schematic of this complexation mechanism is shown in Figure 7. Due to the transport direction of the negatively charged HA, $B(OH)_4^-$ is deposited on the AEMs.

[Figure 7]

3.5. Organic matter membrane deposition

UV-Vis and NPOC measurements showed a decrease in OM within the ED system over the duration of each experiment. The reduction of OM in both diluate and concentrate indicates that the OM is deposited. Figure 8 shows that the mass of OM (mgC) deposited on the AEMs was greater than the mass deposited on the CEMs, which confirms results Lee *et al.* [20]. The negatively

charged HA deposits more readily on the positively charged AEMs in experiments with a higher solution pH. However, Park *et al*. [37] showed that HA has a negative zeta potential in a wide pH range, so that it can foul AEMs in almost the entire pH range. In this study the amount of HA deposited on the AEMs showed a slight decrease with increasing solution pH (from pH 6) (Figure 8A) which cannot be explained by repulsive forces. The macromolecular structures of humic substances influences the properties and affinities of these materials [38]. According to Chen and Schnitzer [39], humic substances behave like uncharged (spherical) polymers at very low pH whereas at high pH, they exhibit polyelectrolytic character of linear shape. Lee *et al*. [17] postulated that the fouling of an AEM is related more to the properties of the foulant (humate) than the electrostatic force between the foulant and the membrane.

[Figure 8]

Unlike HA, the mass of TA deposited on the AEM was pH independent (Figure 8B), with an exception (decrease) at neutral pH. As large molecular weight organics have more difficulty in permeating the AEMs [37], TA, with its lower molecular weight, has increased potential for transportation through the AEM compared to HA.

The mass of AA deposited on the AEMs was lower than HA and TA over the studied pH range (Figure 8C). Avaltroni *et al*. [26] found that the structure of AA follows three pH dependent trends (1) increased aggregation below pH 4 due to a decrease in charge density, (2) molecular expansion between pH 4 and 8 and (3) dissociation above pH 8. The variability seen in the mass above pH 8 could be attributed to AA dissociation.

The AEM surface in contact with the diluate showed visible fouling with HA and TA. This fouling was not reversed by chemical cleaning indicative of strong binding of the OM to the AEM

functional groups and penetration into the membrane. The observed colour change was more pronounced on the area of membranes in contact with ED cell inlets. The fouling of the AEMs was also accompanied by visible swelling. The hydrophobic and hydrophilic acids contained in OM cannot pass through the membranes due to their high molecular weight and it is thought that a fraction of the OM is transported through the membranes as a result of their negative charge density and molecular structure [17, 18]. The surface of the CEMs in contact with both the concentrate and diluate presented little visible evidence of fouling, due to electrostatic repulsion of the negatively charged functional groups within the CEM.

SUVA (L/mg.m) values for HA experiments are shown in Figure 8D. SUVA is used as an indicator for the aromatic content of carbon within a water sample [40]. SUVA values in the diluate and concentrate for the HA experiments were pH and time independent with a values between 2.6 and 5.6 L/mg.m. Shin *et al*. [41] stated that the non-aromatic (aliphatic nature) fractions of HA have a larger molecular size in comparison to the aromatic and carboxylate groups of smaller size fractions. Results from this study, therefore, indicate that ED does not separate the aromatic and non-aromatic fractions of HA.

3.6. ED parameters and performance

An increase in ED stack resistance (see Eqn (2)) was observed at the beginning of the ED process in all experiments as a result of ion depletion within the diluate and membrane boundary layer. An increase in resistance observed at the end of the ED experiments without OM is attributed to the higher demineralization rate in the diluate solution. ED stack resistance as a function of solution pH is shown in Figure 9.

[Figure 9]

The deposition of inorganic trace contaminants and OM on the membranes has implications for ED performance. OM deposition as a foulant layer on and/or inside the membranes increases the resistance at the membrane surface [19, 42]. Between pH 3 and 8 the average stack resistances were indeed greater in the presence of OM; HA (46.3 ± 2.2 Ω), TA (51.3 ± 5.0 Ω) and AA (44.5 ± 1.6 Ω), due to enhanced OM deposition within this pH range (Figure 8). Above pH 8, resistance decreased due to decreased OM membrane deposition.

The performance of the ED process can also be evaluated by the removal of EC (Figure 2D). The average percentage of EC removed without OM was 93.0 ± 2.1 % compared with 91.7 ± 2.5 %, 92.6 ± 3.0 % and 89.4 ± 4.8 % with HA, TA and AA respectively. The presence of OM on the membranes did not significantly lower EC removal. It is possible the OM was loosely packed on the AEM still allowing for the migration of salt ions through the membrane; though at a slightly decreased initial flux (Figure 4D).

4. Conclusions

The purpose of this study was to understand the impact of OM on inorganic contaminant removal. The removal of the contaminants followed the order NO_3^- > F^- > $B(OH)_4^-$. The hydrated radius and subsequent strength of hydration shells is a parameter that plays a significant role in the transport of the ions during ED; as NO_3^- with a smaller hydrated ionic radii and subsequent weaker hydration shell was removed more effectively than F^- with a larger hydrated ionic radii and stronger hydration shell. The transport of $B(OH)_4^-$ in ED was solution pH and hence speciation dependent with increased removal at high pH.

The removal of the inorganic contaminants was enhanced by the presence of OM while the flux decreased indicating mutual dependence of inorganic and organic contaminants in ED. The mechanism for this involves the possible territorial binding and/or complexation of the inorganic

406 contaminants to the negatively charged OM and the subsequent OM deposition on the positively
407 charged AEMs. This membrane deposition led to an increase in stack resistance and a slight
408 reduction in initial EC flux. It is important to study the behaviour of these trace contaminants with
409 OM to better understand the feasibility and applicability of ED for the treatment of real waters.
410

411 **5. Acknowledgements**

412 This work was initially funded through the Australian Research Council (ARC) Linkage Project
413 LP0454254 in collaboration with Brisbane Water along with the ARC Discovery Project
414 DP0559878. The authors thank Eurodia (Germany and France) for the provision of membranes for
415 this project and Berghof (Germany) for the donation of the ED stack. Wytze Meindersma
416 (Eindhoven University of Technology, Netherlands) and Bart van der Bruggen (University of
417 Leuven, Belgium) are acknowledged for helpful discussions. Steffen Zuleeg (EAWAG,
418 Switzerland) and Johannes Fritsch (University of Applied Sciences, Ravensburg-Weingarten,
419 Germany) for help with limiting current density issues. The authors also thank Peter Anderson and
420 Alan Simm (University of Edinburgh, UK) for boron analysis and discussions on boron chemistry
421 and laboratory support, respectively.
422

423 **References**

424 [1] WHO, Guidelines for Drinking Water Quality, World Health Organization, 2006.
425 [2] R. Abu, K. Alsokhny, Geochemical assessment of groundwater contamination with special
426 emphasis on fluoride concentration, North Jordan, Chemie der Erde - Geochem. 64 (2004)
427 171.
428 [3] N. Tamer, B.K. Köroğlu, C. Arslan, M. Akdoğan, M. Köroğlu, H. Çam, M. Yildiz,
429 Osteosclerosis due to endemic fluorosis, Sci. Total Environ. 373 (2007) 43.
430 [4] M. Zeni, R. Riveros, K. Melo, R. Primieri, S. Lorenzini, Study on fluoride reduction in
431 artesian well-water from electrodialysis process, Desalination. 185 (2005) 241.

[5] A. Elmidaoui, F. Elhannouni, M. Taky, L. Chay, M.A. Menkouchi Sahli, L. Echihabi, M. Hafsi, Optimization of nitrate removal operation from ground water by electrodialysis, Sep. Purif. Technol. 29 (2002) 235.

[6] Council Directive 98/83/EC of 3 November 1998 on the quality of water intended for human consumption, *Official Journal L* 330, European Union, 1998, pp. 32-54.

[7] NHMRC, Australian Drinking Water Guidelines, National Health and Medical Research Council, Canberra, 2004.

[8] K. Kesore, F. Janowski, V.A. Shaposhnik, Highly effective electrodialysis for selective elimination of nitrates from drinking water, J. Membr. Sci. 127 (1997) 17.

[9] J.M. Ortiz, J.A. Sotoca, E. Exposito, F. Gallud, V. Garcia-Garcia, V. Montiel, A. Aldaz, Brackish water desalination by electrodialysis: batch recirculation operation modeling, J. Membr. Sci. 252 (2005) 65.

[10] M. Turek, P. Dydo, J. Trojanowska, B. Bandura, Electrodialytic treatment of boron-containing wastewater, Desalination. 205 (2007) 185.

[11] L. Melnyk, V. Goncharuk, I. Butnyk, E. Tsapiuk, Boron removal from natural and wastewaters using combined sorption/membrane process, Desalination. 185 (2005) 147.

[12] L. Melnik, O. Vysotskaja, B. Kornilovich, Boron behavior during desalination of sea and underground water by electrodialysis, Desalination. 124 (1999) 125.

[13] Z. Yazicigil, Y. Oztekin, Boron removal by electrodialysis with anion-exchange membranes, Desalination. 190 (2006) 71.

[14] J.A. Dean, Lange's handbook of chemistry, McGraw-Hill, New York, 1999.

[15] F.H. Frimmel, Characterization of natural organic matter as major constituents in aquatic systems, J. Contam. Hydrol. 35 (1998) 201.

[16] D. Hayes, J. Carter, T.J. Manning, Fluoride binding to humic acid, J. Radioanal. Nucl. Chem. Lett. 201 (1995) 135.

457 [17] H.J. Lee, D.H. Kim, J. Cho, S.H. Moon, Characterization of anion exchange membranes
458 with natural organic matter (NOM) during electrodialysis, Desalination. 151 (2002) 43.
459 [18] D.H. Kim, S.H. Moon, J. Cho, Investigation of the adsorption and transport of natural
460 organic matter (NOM) in ion-exchange membranes, Desalination. 151 (2002) 11.
461 [19] J.S. Park, J.H. Choi, K.H. Yeon, S.H. Moon, An approach to fouling characterization of an
462 ion-exchange membrane using current-voltage relation and electrical impedance
463 spectroscopy, J. Colloid Interface Sci. 294 (2006) 129.
464 [20] H.J. Lee, J.H. Choi, J. Cho, S.H. Moon, Characterization of anion exchange membranes
465 fouled with humate during electrodialysis, J. Membr. Sci. 203 (2002) 115.
466 [21] A. Koparal, U. Ogutveren, Removal of nitrate from water by electroreduction and
467 electrocoagulation, J. Hazard. Mater. 89 (2002) 83.
468 [22] Y.P. Chin, G. Aiken, E. O'Loughlin, Molecular Weight, Polydispersity, and Spectroscopic
469 Properties of Aquatic Humic Substances, Environ. Sci. Technol. 28 (1994) 1853.
470 [23] T. Shutava, M. Prouty, pH responsive decomposable layer-by-layer nanofilms and capsules
471 on the basis of tannic acid, Macromolecules. 38 (2005) 2850.
472 [24] J.H. An, S. Dultz, Adsorption of tannic acid on chitosan-montmorillonite as a function of pH
473 and surface charge properties, Appl. Clay Sci. 36 (2007) 256.
474 [25] T. Coradin, J. Livage, Synthesis and characterization of alginate/silica biocomposites, J. Sol-
475 Gel Sci. Technol. 26 (2003) 1165.
476 [26] F. Avaltroni, M. Seijo, S. Ulrich, S. Stoll, K.J. Wilkinson, Conformational Changes and
477 Aggregation of Alginic Acid as Determined By Fluorescence Correlation Spectroscopy,
478 Biomacromolecules. 8 (2007) 106.
479 [27] L.A. Richards, B.S. Richards, H.M.A. Rossiter, A.I. Schäfer, Impact of speciation on
480 fluoride, arsenic and magnesium retention by nanofiltration/reverse osmosis in remote
481 australian communities, Desalination. Accepted (2009).

[28] L.A. Richards, B.S. Richards, H.M.A. Rossiter, A.I. Schäfer, Impact of speciation on fluoride, arsenic and magnesium retention by nanofiltration/reverse osmosis in remote australian communities, Desalination. In press (2008).

[29] B.B. Owen, E.J. King, The Effect of Sodium Chloride upon the Ionization of Boric Acid at Various Temperatures, J. Amer. Chem. Soc. 65 (1943) 1612.

[30] B. Tansel, J. Sager, T. Rector, J. Garland, R.F. Strayer, L. Levine, M. Roberts, M. Hummerick, J. Bauer, Significance of hydrated radius and hydration shells on ionic permeability during nanofiltration in dead end cross flow modes, Sep. Purif. Technol. 51 (2006) 40.

[31] A.G. Volkov, S. Paula, D.W. Deamer, Two mechanisms of permeation of small neutral molecules and hydrated ions across phospholipid bilayers, Bioelectrochem. Bioenerg. 42 (1997) 153.

[32] H. Strathmann, Ion-exchange membrane separation processes, Elsevier, Amsterdam, Netherlands, 2004.

[33] P.W. Atkins, Physical chemistry, Oxford University Press, Oxford, 1990.

[34] H.R. Schulten, M. Schnitzer, Three-dimensional models for humic acids and soil organic matter, Naturwissenschaften. 82 (1995) 487.

[35] E. Chauveheid, M. Denis, The boron–organic carbon correlation in water, Water Research. 38 (2004) 1663–1668.

[36] P. Schmitt-Kopplin, N. Hertkorn, A.W. Garrison, D. Freitag, A. Kettrup, Influence of Borate Buffers on the Electrophoretic Behavior of Humic Substances in Capillary Zone Electrophoresis, Anal. Chem. 70 (1998) 3798.

[37] J.S. Park, H.J. Lee, S.J.G. Choi, K.E., J. Cho, S.H. Moon, Fouling mitigation of anion exchange membrane by zeta potential control, J. Colloid Interface Sci. 259 (2003) 293.

[38] K. Ghosh, M. Schnitzer, Macromolecular structures of humic substances, Soil Science. 129 (1980) 266.

508 [39] Y. Chen, M. Schnitzer, Viscosity measurements on soil humic substances, Soil Sci. Soc.
509 Am. J. 40 (1976) 866.
510 [40] J.P. Croué, D. Violleau, C. Bodaire, B. Legube, Removal of hydrophobic and hydrophilic
511 constituents by anion exchange resin, Water Sci. Technol. 40 (1999) 207.
512 [41] H.S. Shin, J.M. Monsallier, G.R. Choppin, Spectroscopic and chemical characterizations of
513 molecular size fractionated humic acid, Talanta. 50 (1999) 641.
514 [42] V. Lindstrand, G. Sundstrom, A.S. Jonsson, Fouling of electrodialysis membranes by
515 organic substances, Desalination. 128 (2000) 91.
516 [43] M.Y. Kiriukhin, K.D. Collins, Dynamic hydration numbers for biological important ions,
517 Biophys. Chem. 99 (2002) 155.
518 [44] K.D. Collins, Sticky ions in biological systems, Proc. Natl. Acad. Sci. US. 92 (1995) 5553.
519 [45] L. Pauling, The nature of the chemical bond and the structure of molecules and crystals: An
520 introduction to modern structural chemistry, Cornell University Press, New York, 1960.
521 [46] H. Corti, R. Crovetto, R. Fernandez-Prini, Mobilities and ion-pairing in $LiB(OH)_4$ and
522 $NaB(OH)_4$ aqueous solutions. A conductivity study, J. Sol. Chem. 9 (1980) 617.
523 [47] Y. Marcus, Thermodynamics of solvation of ions Part 5.- Gibbs free energy of hydration at
524 298.15 K, J. Chem. Soc. Faraday Trans. 87 (1991) 2995.
525 [48] R.A. Robinson, R.H. Stokes, Electrolyte solutions, Butterworths, London, 1970.
526 [49] Y.P. Chin, G. Aiken, K.M. Danielsen, Binding of pyrene to aquatic and commercial humic
527 substances: The role of molecular weight and aromaticity, Environ. Sci. Technol. 31 (1997)
528 1630.
529 [50] M. Fukushima, S. Tanaka, H. Nakamura, S. Ito, Acid-base characterization of molecular
530 weight fractionated humic acid, Talanta. 43 (1996) 383.
531 [51] G.R. Choppin, P.M. Shanbhag, Binding of calcium by humic acid, J. Inorg. Nucl. Chem. 43
532 (1981) 921.

[52] M. Terashima, M. Fukushima, S. Tanaka, Influence of pH on the surface activity of humic acid: micelle-like aggregate formation and interfacial adsorption, Colloids Surf., A. 247 (2004) 77.

[53] H.R. Schulten, A chemical structure for Humic Acid. Pyrolysis-gas chromatography/mass spectrometry and pyrolysis-soft ionization mass spectrometry evidence, in: N. Senesi, T.M. Miano, (Eds), Humic substances in the global environment and implications on human health, Elsevier Science, 1994, pp. 43-56.

List of Tables

547 Table 1

Parameter	Unit	Na^+	Cl^-	F^-	NO_3^-	$B(OH)_4^-$	References
Crystal ionic radii, *r*	nm	-	-	0.116 - 0.119	0.179 - 0.189	0.244-0.261	[30, 31, 43-46]
		0.117	0.164	0.133 - 0.135	0.206		[45, 47]
Hydrated ionic radii, Δ*r*	nm	0.358	0.332	0.352	0.340	[a]	[31]
Number of water molecules in hydration shell, *n*	-	3.5	2.0	2.7	2.0	[a]	[47]
Molar Gibbs energy of hydration, $\Delta_{hyd} G^*_{calc}$	kJ/mol	-385	-270	-345	-275	[a]	[47]
Ion mobility at 25°C, *u*	m^2/sV	5.19	7.91	5.70	7.40	[a]	[33]
Ion equivalent conductivity, λ°equiv	$cm^2/\Omega equiv$	50.1	76.4	55.4	71.5	[a]	[48]

548 [a] Data not available.

549 Table 2

Organic Type	Category	Origin	Molecular Formulae	MW (g/mol)	Carbon (%)	p*Ka*	Charge			References
							Acidic pH	Neutral pH	Basic pH	
Humic Acid (HA)	OM surrogate	Soil	$C_{342}H_{388}O_{124}N_5$ [a]	4100	56	3.5-5.04	Neutral	Negative	Negative	[22, 34, 41, 49-52]
Tannic Acid (TA)	Polyphenol	Plants	$C_{76}H_{52}O_{46}$	1701	54	2.5-10	Neutral	Negative	Negative	[23]
Alginic Acid (AA)	Polysaccharide	Brown seaweed and algae	$[C_6H_8O_6]_n$	21000	36	2.0-3.5	Negative	Negative	Negative	[26]

550 [a] Based on model by [53]. [b] Sigma Aldrich Humic Acid.

List of Figures

577 Figure 1

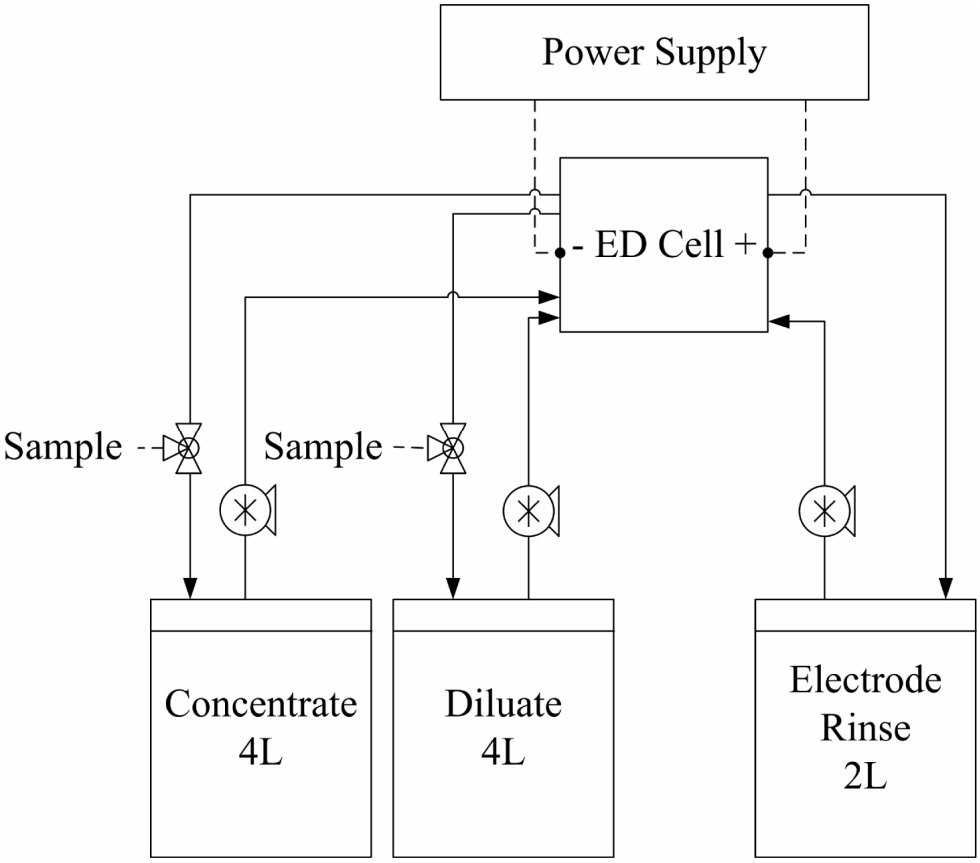

578

579 Figure 2

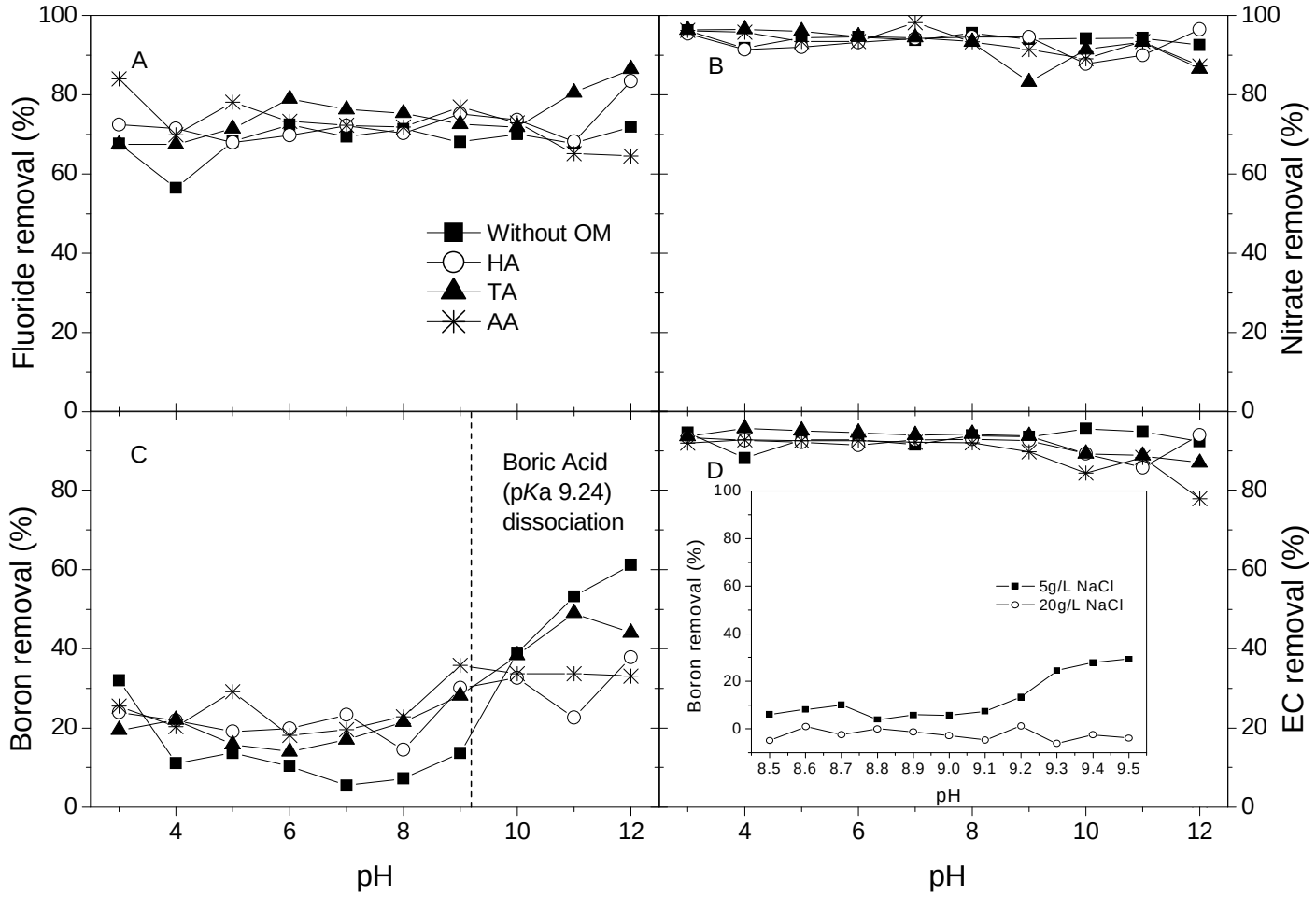

580

581 Figure 3

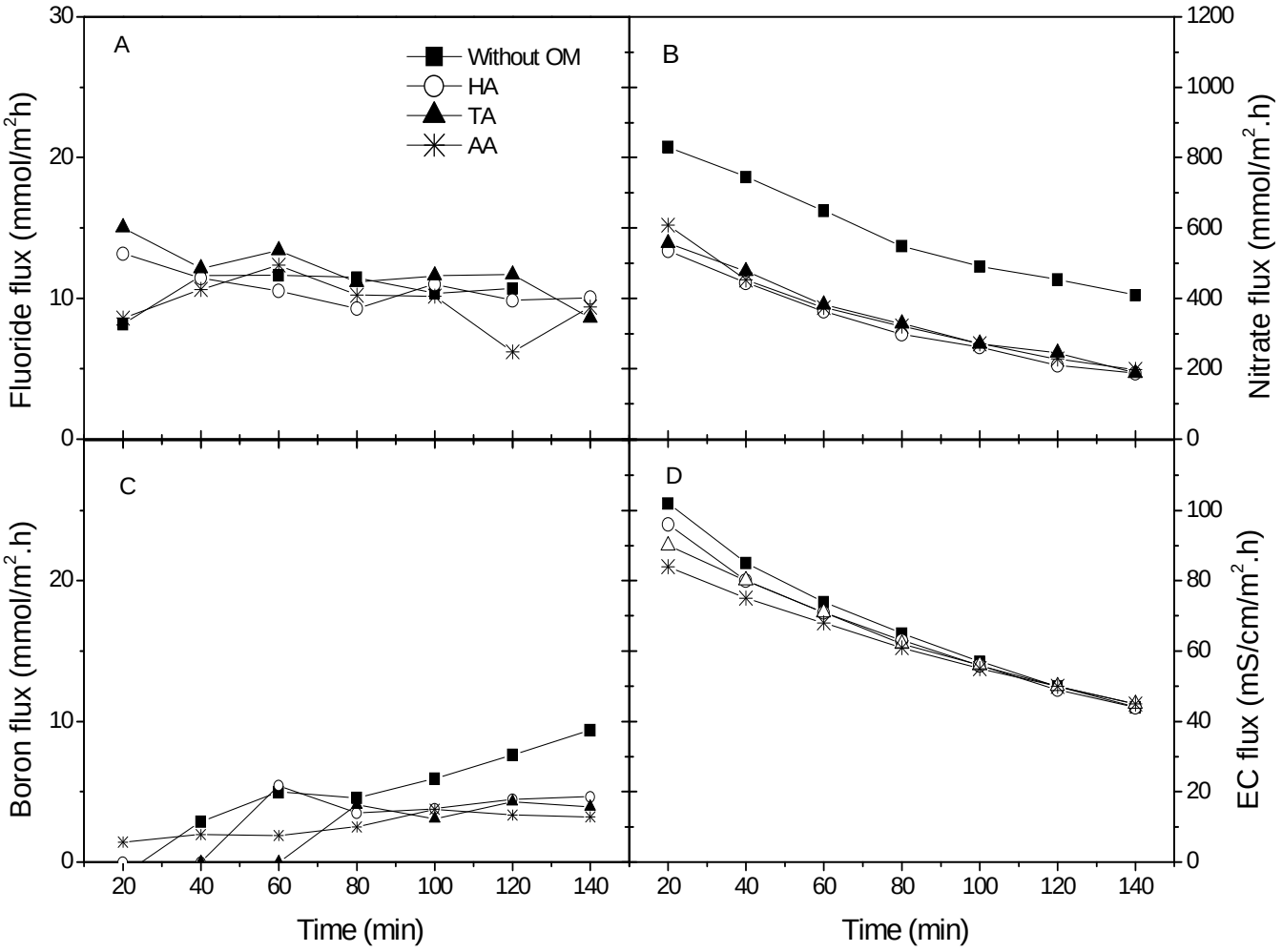

582

583 Figure 4

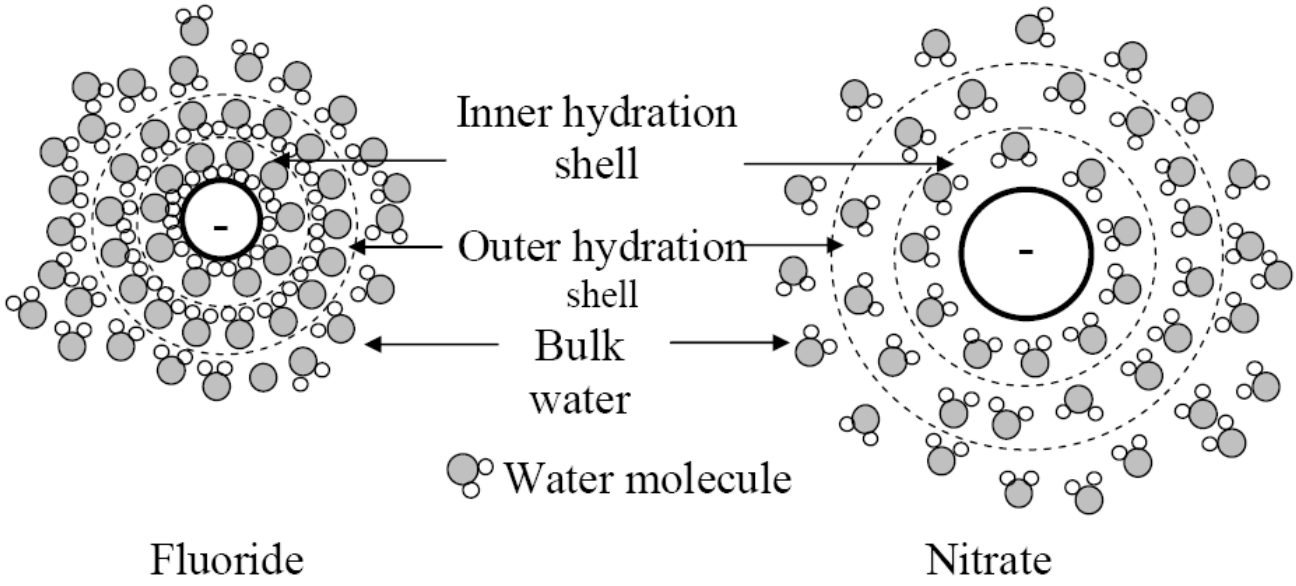

584

585 Figure 5

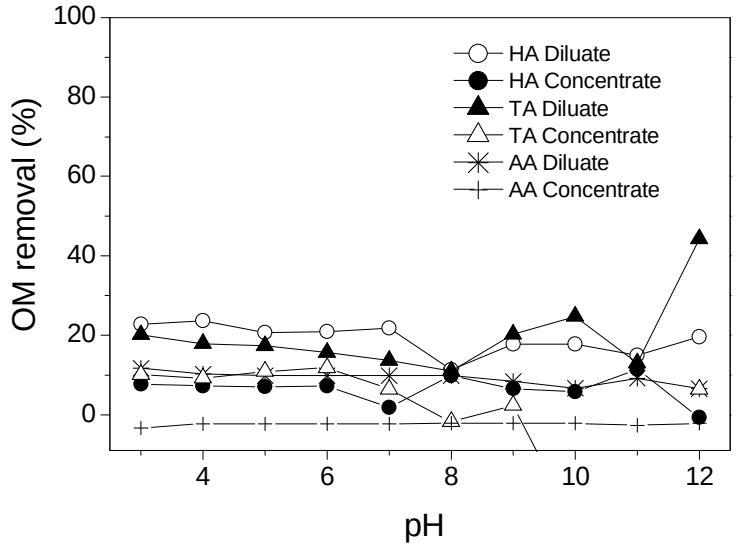

586

587 Figure 6

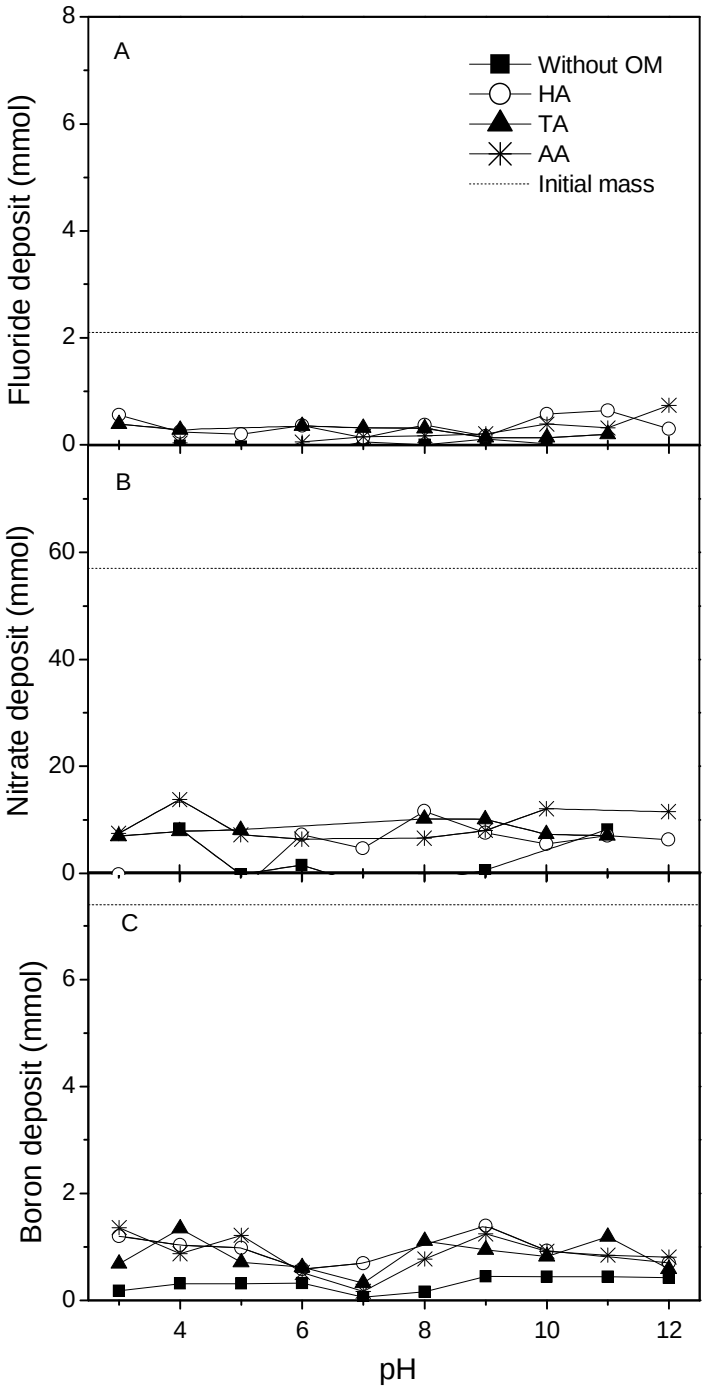

588

589 Figure 7

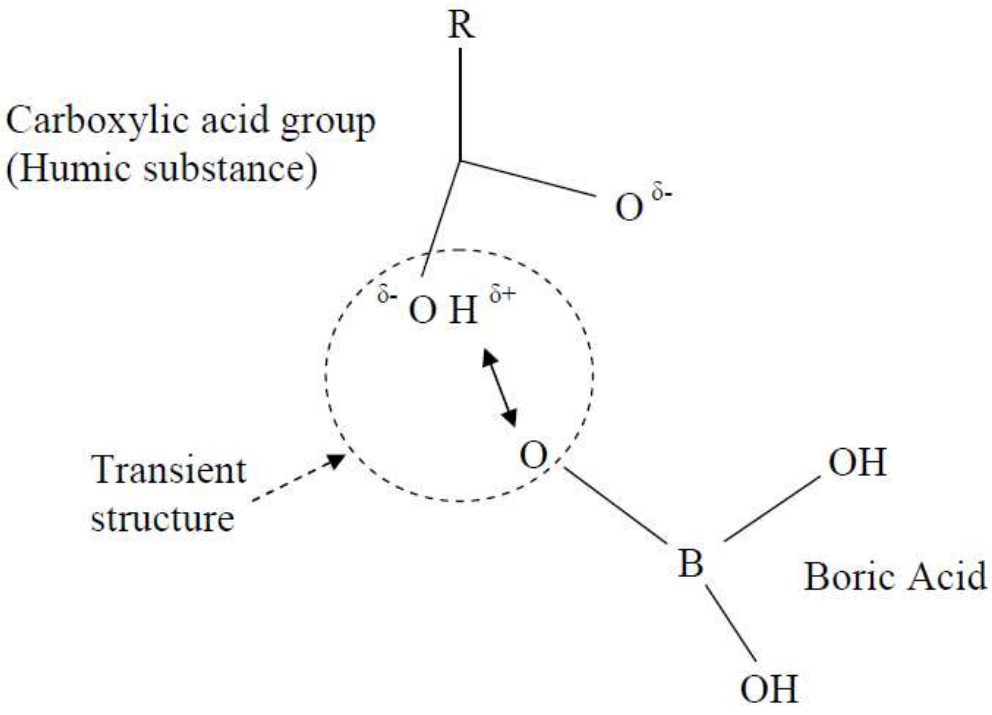

590

591 Figure 8

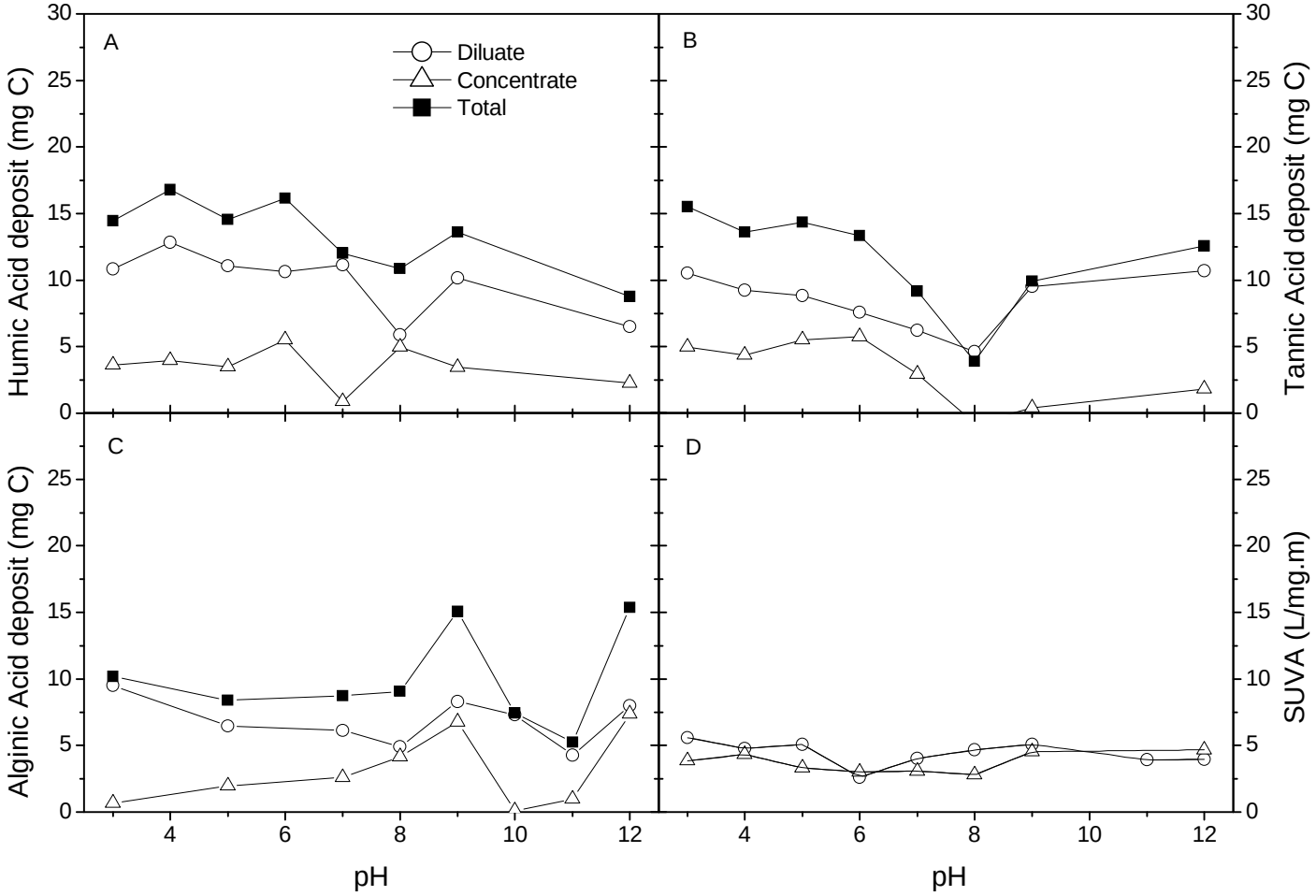

592

593 Figure 9

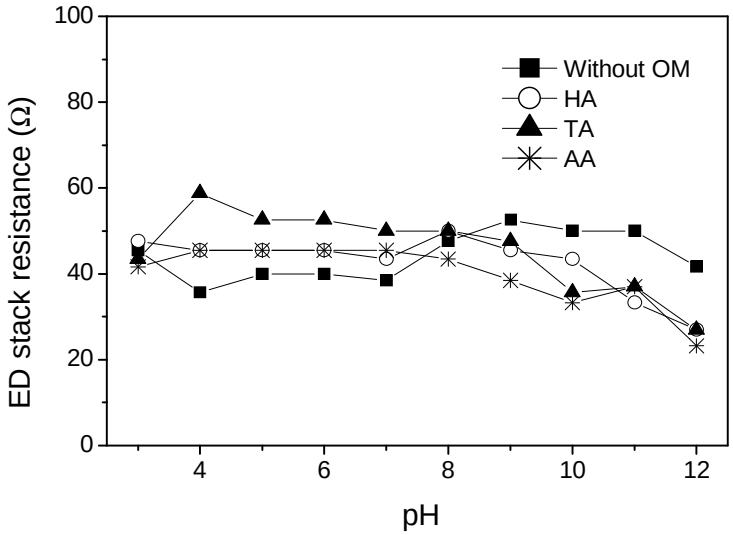

594